A Molecular Link between Activation and Inactivation of Sodium Channels

MICHAEL E. O'LEARY,* LI-QIONG CHEN,‡ ROLAND G. KALLEN,‡ and RICHARD HORN*

From the *Department of Physiology, Jefferson Medical College, Philadelphia, Pennsylvania 19107; ‡Department of Biochemistry and Biophysics, University of Pennsylvania School of Medicine, Philadelphia, Pennsylvania 19104-6059

ABSTRACT A pair of tyrosine residues, located on the cytoplasmic linker between the third and fourth domains of human heart sodium channels, plays a critical role in the kinetics and voltage dependence of inactivation. Substitution of these residues by glutamine ($Y^{1494}Y^{1495}$/QQ), but not phenylalanine, nearly eliminates the voltage dependence of the inactivation time constant measured from the decay of macroscopic current after a depolarization. The voltage dependence of steady state inactivation and recovery from inactivation is also decreased in YY/QQ channels. A characteristic feature of the coupling between activation and inactivation in sodium channels is a delay in development of inactivation after a depolarization. Such a delay is seen in wild-type but is abbreviated in YY/QQ channels at −30 mV. The macroscopic kinetics of activation are faster and less voltage dependent in the mutant at voltages more negative than −20 mV. Deactivation kinetics, by contrast, are not significantly different between mutant and wild-type channels at voltages more negative than −70 mV. Single-channel measurements show that the latencies for a channel to open after a depolarization are shorter and less voltage dependent in YY/QQ than in wild-type channels; however the peak open probability is not significantly affected in YY/QQ channels. These data demonstrate that rate constants involved in both activation and inactivation are altered in YY/QQ channels. These tyrosines are required for a normal coupling between activation voltage sensors and the inactivation gate. This coupling insures that the macroscopic inactivation rate is slow at negative voltages and accelerated at more positive voltages. Disruption of the coupling in YY/QQ alters the microscopic rates of both activation and inactivation.

INTRODUCTION

Voltage-dependent sodium channels are responsible for the rising phase of the action potential in nerve and muscle cells. Depolarization causes an increase in the rate of activation, leading to the opening of channels, and an increase in the rate of inactivation, which subsequently closes the channels (for reviews see Armstrong, 1981; Bezanilla, 1985; Patlak, 1991; Sigworth, 1993; Keynes, 1994). The coordination between activation and inactivation insures that the action potential can be

Address correspondence to Richard Horn, Department of Physiology, Jefferson Medical College, 1020 Locust Street, Philadelphia, PA 19107.

J. GEN. PHYSIOL. © The Rockefeller University Press · 0022-1295/95/10/641/18 $2.00
Volume 106 October 1995 641–658

triggered reliably and will be brief, and also that sodium channels will recover appropriately from inactivation after an action potential. Activation derives its voltage dependence from the movement of charges within the membrane electric field. Early studies of the sodium current in squid axon modeled inactivation as a separate voltage-dependent process, independent of activation (Hodgkin and Huxley, 1952). However it is generally believed now that inactivation derives most of its voltage dependence from being coupled to activation. According to this idea, depolarization causes voltage-dependent activation gates to open, and the rate of inactivation increases as a consequence of these conformational changes in the channel protein.

The abolition of inactivation by cytoplasmic endopeptidases (Rojas and Armstrong, 1971) has spawned the idea that the inactivation gate is a cytoplasmic region of the sodium channel protein that blocks the pore when it is in its binding site. Mutagenesis studies (Stühmer, Conti, Suzuki, Wang, Noda, Yahagi, Kubo, and Numa, 1989; Moorman, Kirsch, Brown, and Joho, 1990; Patton, West, Catterall, and Goldin, 1992) suggest that this gate is located within a 53–amino acid loop between the third and fourth homologous domains, the D3–D4 linker (Fig. 1 *A*). A three amino acid motif in this linker, IFM (isoleucine-phenylalanine-methionine), is conserved in all cloned sodium channels and is critical for normal inactivation (West, Patton, Scheuer, Wang, Goldin, and Catterall, 1992; Hartmann, Tiedeman, Chen, Brown, and Kirsch, 1994). Substitution of these amino acids by glutamine abolishes rapid inactivation. The most important member of this hydrophobic trio is the aromatic residue phenylalanine. By contrast, glutamine substitution for the 11 lysines in the D3–D4 linker has less effect (Moorman et al., 1990; West et al., 1992), indicating that these positively charged residues do not play a critical role in the inactivation of sodium channels. There are six other aromatic residues, either phenylalanines or tyrosines, in the D3–D4 linker of cardiac sodium channels (Rogart, Cribbs, Muglia, Kephart, and Kaiser, 1989; Gellens, George, Chen, Chahine, Horn, Barchi, and Kallen, 1992). We have mutated the two adjacent tyrosines in close proximity to IFM (Fig. 1 *A*), in the human heart sodium channel (hH1; Gellens et al., 1992), to determine whether these aromatic residues contribute to inactivation. Mutations of these tyrosines affect the kinetics of both activation and inactivation, suggesting that they play an important role in the coupling between activation and inactivation.

METHODS

Mutagenesis and Transfection

For preparation of mutants a 399-bp KpnI-BstEII fragment (4228–4627 nt) from hH1 was subcloned into pSelect-1 (pS1/399). Site-directed mutagenesis was performed with a Promega kit according to the directions of the manufacturer (Promega Corp., Madison, WI). The following phosphorylated antisense mutagenic oligonucleotides (altered sites are in bold underlining) were used (1.25 pmol each):

YY1494/1495FF:5′-TTCTTCATGGCATTG**A**AG**A**ACTTCTTCTGCTCCT-3′
Y1494F:5′-ATGGCATTGTAG**A**ACTTCTTCTGCT-3′
Y1495F:5′-TTCATGGCATTG**A**AGTACTTCTTCT-3′

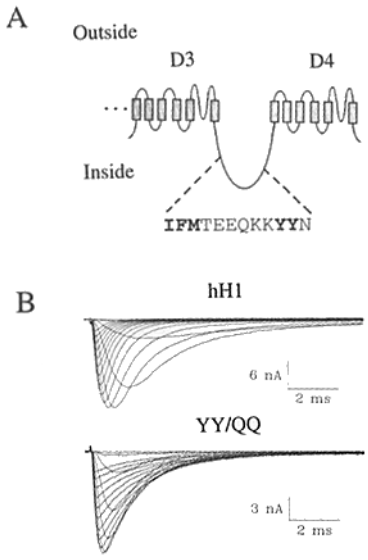

FIGURE 1. Effect of mutations of Y1494 and Y1495 on hH1 sodium currents. (*A*) Diagram of the D3–D4 linker showing the IFM and YY residues boxed in bold. (*B*) Sodium currents from WT- and YY/QQ-transfected tsA201 cells activated by depolarizations in 10-mV increments from −80 to +70 mV; holding potential, −120 mV.

YY1494/1495QQ: 5′-CTTCTTCATGGCATTCTGCTGCTTCTTCTGCTCCTC-3′
Y1494Q: 5′-CTTCATGGCATTGTACTGCTTCTTCTGCTCCTC-3′
Y1495Q: 5′-CTTCTTCATGGCATTCTGGTACTTCTTCTGCTC-3′.

The candidate clones were screened by nucleotide sequencing. The 399-bp KpnI-BstEII fragment carrying the mutation was isolated from pS1/399 and substituted for the wild-type KpnI and BstEII segment of hH1 contained in the pCDNA-1 vector (Invitrogen Corp., San Diego, CA). All final recombinant DNA constructs were confirmed by nucleic acid sequencing.

Standard methods of transient calcium phosphate transfection of tsA201 cells were used (Margolskee, McHendry-Rinde, and Horn, 1993). Approximately 50% of cells expressed large Na currents (>500 pA at −10 mV) in typical experiments. Recordings were obtained 1–3 d after transfection.

Electrophysiology and Data Analysis

Standard whole-cell recording methods, including 80% compensation for series resistance, were used (O'Leary and Horn, 1994). Series resistance errors were <3 mV, and the expected charging time constant for the cells was <10 μs. Patch electrodes contained (in millimolar): 150 CsF, 10 EGTA, 10 Cs-HEPES, pH 7.3. The bath contained 150 NaCl, 2 KCl, 1.5 $CaCl_2$, 1 $MgCl_2$, 10 Na-HEPES, pH 7.3. The recording amplifier was an Axopatch 200A (Axon Instruments, Inc., Burlingame, CA); data were filtered at 5–10 kHz and acquired using pCLAMP (Axon Instruments Inc.). Temperature was changed with Peltier units using a TC-10 controller (Dagan Corp, Minneapolis, MN). Except where indicated, experiments were performed at 21–23°C. Whole-cell data were analyzed by a combination of pCLAMP programs, SigmaPlot (Jandel Scientific, San Rafael, CA), and our own FORTRAN programs. Data are presented as mean ± SEM.

Cell-attached experiments at room temperature, 21–23°C, used a bath solution (in millimolar): 100 K methylsulfate, 50 KCl, 1.5 $CaCl_2$, 1 $MgCl_2$, 10 K-HEPES, pH 7.4. The pipette solution was 150 NaCl, 10 tetraethylammonium Cl, 0.0001 tetrodotoxin, 2 KCl, 1.5 $CaCl_2$, 1 $MgCl_2$, 10 Na-HEPES, pH 7.3. Data were filtered at 5 kHz, sampled at 25 kHz, digitally filtered again at 3 kHz, idealized using TRANSIT (Dr. A. VanDongen, Duke University, Durham, NC), and further ana-

lyzed using our own FORTRAN programs (Chahine, George, Zhou, Ji, Sun, Barchi, and Horn, 1994). The effective dead time for a detectable transition was ~70 μs.

RESULTS

Loss of Voltage Dependence of Inactivation in Tyrosine Mutants

Fig. 1 *B* shows families of whole-cell sodium currents from wild-type (WT) hH1 and from a mutant in which two tyrosines, Y1494 and Y1495, are substituted by glutamine (YY/QQ). The mutant and WT channels were expressed transiently in the tsA201 cell line. Both clones show a typical pattern of rapid voltage-dependent activation followed by a slower inactivation. However, the YY/QQ mutant inactivates more rapidly than WT at voltages more negative than −30 mV and more slowly than WT at positive voltages. In both WT and mutant channels the decay of the current after a depolarization is well-fit by a single exponential function at all voltages, with time constants (τ_h) plotted in Fig. 2 *A*. The WT τ_h is strongly voltage dependent, especially over the voltage range where sodium channels open (Fig. 5). By contrast, τ_h of the YY/QQ mutant is almost completely insensitive to voltage between −50 and +70 mV. YY/QQ mutations also decrease the voltage dependence of steady state inactivation (Fig. 2 *B*) by an equivalent loss of 1.8 electronic (e_0) charges. In addition, this double mutation speeds the recovery from inactivation and decreases its voltage dependence (Fig. 2, *C* and *D*), showing that these residues are important for both entry into and exit from inactivated states. The data suggest that these two tyrosines contribute to the coupling between activation and inactivation, and that glutamines in these positions disrupt the coupling mechanism.

The aromatic side chains of tyrosines may be necessary for the normal function of this coupling mechanism, because phenylalanine substitutions for tyrosine (YY/FF) have little effect on τ_h, steady state inactivation, or recovery from inactivation (Fig. 2). Single substitutions, Y1494Q or Y1495Q, have less effect on τ_h than the double mutation (Fig. 2 *A*), suggesting that the two tyrosines work in concert to promote a normal voltage dependence of inactivation.

Steady state inactivation depends on the rate constants for entry into and exit from inactivated states. The time constant of recovery from inactivation (τ_{rec}) provides information on the rate of leaving inactivated states at negative voltages. τ_{rec} is significantly smaller in YY/QQ than in WT (Fig. 2, *C* and *D*). Because the midpoint of steady state inactivation is comparable for WT and YY/QQ (Fig. 2 *B*), the rate of entering an inactivated state must be greater in YY/QQ than in WT at voltages over which steady state inactivation changes. We tested this prediction by measuring the reduction in peak current after a variable-duration conditioning pulse to voltages from −90 to −30 mV (Fig. 3 *B*, *inset*). Fig. 3, *A* and *B*, show that depolarizing prepulses cause a voltage-dependent inactivation in both WT and YY/QQ. The data were reasonably fit by single exponential decays, as shown, and the time constants (τ_c) are plotted in Fig. 3 *C* (*filled symbols*), along with the τ_h values from Fig. 2 *A* (*open symbols*). Fig. 3 *C* shows that the rate of entry into inactivated states is voltage dependent, for both WT and YY/QQ, between −30 and −90 mV, with the absolute rates being greater for YY/QQ than for WT channels, in accordance with the above prediction. The WT time constant is more voltage dependent, increasing 57-fold

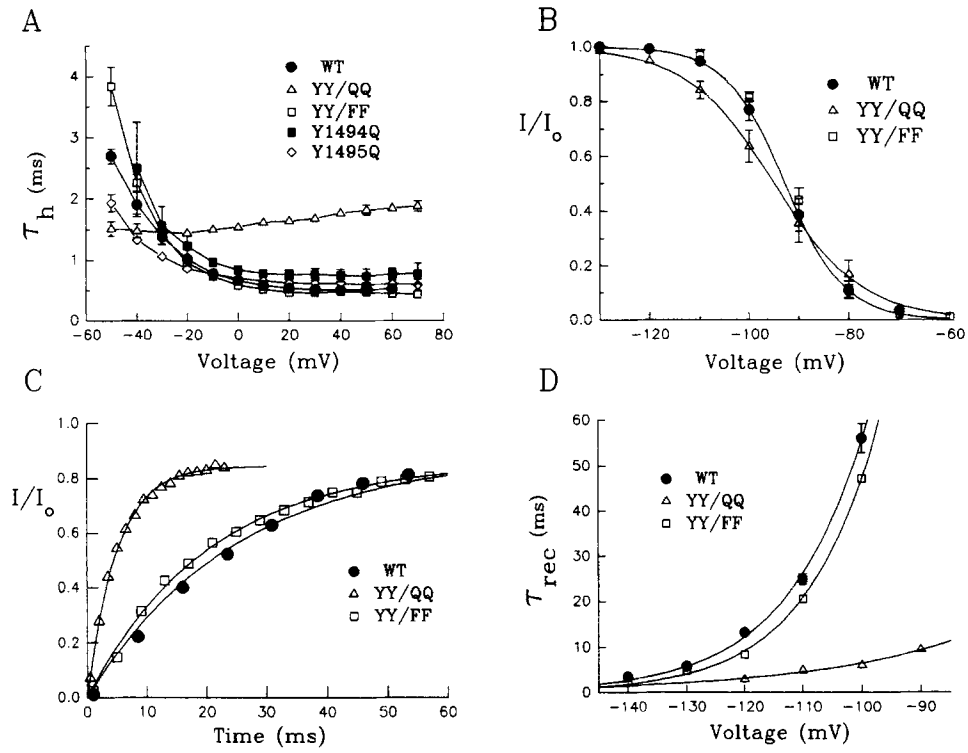

FIGURE 2. Effect of mutations of Y1494 and Y1495 on inactivation. (*A*) τ_h vs voltage for WT and mutant channels. (*B*) Steady state inactivation induced by a 500-ms prepulse to the indicated voltage. Holding potential, −120 mV. The best-fit Boltzmann curves have slopes of 5.7 ± 0.1 mV (*WT*), 8.9 ± 0.2 mV (*YY/QQ*), and 5.6 ± 0.1 mV (*YY/FF*). The midpoints are −92.1 ± 0.1 mV (*WT*), −95.0 ± 0.2 mV (*YY/QQ*), and −91.5 ± 0.1 mV (*YY/FF*). (*C*) Recovery from inactivation at −110 mV. Inactivation induced by a 15-ms prepulse to −20 mV, followed by a variable duration recovery at −110 mV, and tested by a depolarization to −20 mV. The time course of recovery was fit by a single exponential for each clone. (*D*) Time constants for recovery from inactivation. Recovery time course at the indicated voltage was fit with a time constant, τ_{rec}. The smooth curves plot the exponential voltage dependence of τ_{rec}: *e*-fold/13.2 mV (*WT*), *e*-fold/27.3 mV (*YY/QQ*), *e*-fold/12.3 mV (*YY/FF*).

over this range, compared to only 13-fold for YY/QQ. This reduction in voltage dependence of the rate of inactivation for YY/QQ should contribute to the decreased slope of the steady state inactivation curve (Fig. 2 *B*).

A comparison of the time constant of inactivation induced by a prepulse (τ_c) and the current decay during a single pulse (τ_h) yields a surprising result. In WT channels these time constants are comparable in the voltage range where our measurements overlap (Fig. 3 *C*). YY/QQ inactivation time constants, however, differ markedly for one- and two-pulse protocols. The two-pulse time constant of YY/QQ is smaller and more voltage dependent than τ_h, showing a fundamental difference between these two indicators of inactivation rate. The two-pulse time constant τ_c represents the time required for inactivation of sodium channels during the

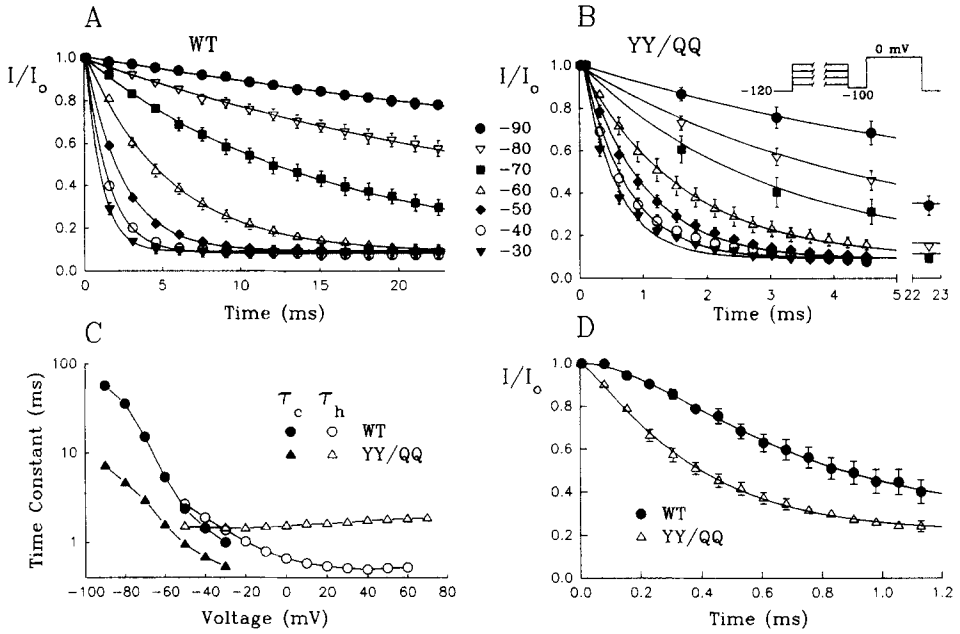

FIGURE 3. Time course of two-pulse inactivation. Voltage protocol in inset above *B*. Peak current amplitude at a test pulse to 0 mV is measured as a function of the duration of a conditioning pulse. A 1-ms prepulse to −100 mV resets activation gates without significantly allowing channels to recover from inactivation (Gillespie and Meves, 1980; Goldman and Kenyon, 1982). (*A*) WT and (*B*) YY/QQ normalized amplitude of peak current in the test pulse is plotted against the duration of conditioning pulses betwen −90 mV (*filled circles*) and −30 mV (*filled triangles*) in 10-mV increments. The data are fit by single exponential relaxations with time constants τ_c. (*C*) τ_c from *A* and *B* are plotted vs conditioning pulse voltage as filled symbols. For comparison the τ_h values from Fig. 2 *A* are also plotted as open symbols. (*D*) Two-pulse inactivation for a −30 mV conditioning pulse, plotted on an expanded time base. The smooth curves are fits to a single exponential relaxation raised to a power. The best fit time constants are 481 ± 46 ms (*WT*) and 323 ± 17 ms (*YY/QQ*), and the powers are 2.10 ± 0.10 (*WT*) and 1.31 ± 0.06 (*YY/QQ*). Data for five WT and six YY/QQ cells are shown.

prepulse, whereas the single-pulse τ_h reflects the inactivation only of the subset of channels that are opened by the depolarization. The voltage dependence of τ_c in YY/QQ, therefore, primarily derives from channels that never reach an open state, i.e., that inactivate from closed states. Because τ_c is smaller than τ_h in YY/QQ, and because the mutant τ_c is smaller than WT τ_c, our data suggest that the microscopic rate constants for inactivating from closed states are enhanced by the YY/QQ mutations.

One of the expected consequences of a coupling between activation and inactivation is that inactivation cannot occur instantaneously after a step depolarization, but only after a lag (Goldman and Schauf, 1972; Bezanilla and Armstrong, 1977). Fig. 3 *D* shows that such a lag is present in WT channels at −30 mV, but is markedly reduced in YY/QQ. A sigmoidal lag in the time course of inactivation in the WT is

reminiscent of the lag in opening of sodium channels after a step depolarization, suggesting that inactivation occurs after one or more conformational transitions among closed states of the activation pathway. The abbreviated delay of YY/QQ channels is evidence that they inactivate more readily from closed states near the beginning of the activation pathway. An alternative possibility, which we discuss below, is that YY/QQ mutations, although on the putative inactivation gate, speed the rate of activation at negative voltages.

The relationship between the macroscopic rates and steady state values of inactivation is remarkably simple for WT channels, as shown in Fig. 4 *A*. If the entry and exit from inactivation behaves like a two-state first-order reaction, as envisaged by Hodgkin and Huxley (1952), steady state inactivation can be predicted uniquely from the kinetics. If α_I and β_I represent the voltage-dependent rate constants for leaving and entering an inactivated state, respectively, the time constants for recovery from inactivation (τ_{rec}) and two-pulse inactivation (τ_c) should be equivalent at any voltage, and will equal $(\alpha_I + \beta_I)^{-1}$. Furthermore, steady state inactivation (e.g., Fig. 2 *B*) is the steady state probability of not being inactivated, which equals $\alpha_I/(\alpha_I + \beta_I)$ at any voltage. Plots of τ_{rec}, τ_c, and steady state inactivation are superimposed in Fig. 4. The rate constants α_I and β_I were assumed to have an exponential dependence on membrane potential. The WT time constants are well-fit by this simple, two-state model (the bell-shaped curve in Fig. 4 *A*), and the estimated values of α_I and β_I at

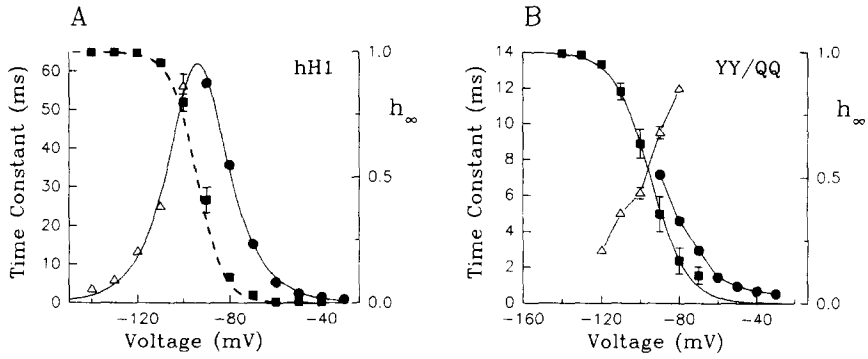

FIGURE 4. Rates and equilibrium of inactivation. Steady state probability of not being inactivated (*closed squares*), τ_c (*closed circles*), and τ_{rec} (*open triangles*) plotted against membrane potential. (*A*) WT channels. τ_c and τ_{rec} were simultaneously fit (*bell-shaped curve*) with a two-state model described in the text. The rate constants α_I and β_I for the model each have an exponential voltage dependence. The best fit values for these rates (1/ms) are:

$$\alpha_I = 1.67 \times 10^{-6} \exp(-2.25\ V/25), \text{ and} \quad (1)$$

$$\beta_I = 26.2 \exp(2.15\ V/25), \quad (2)$$

where V is membrane potential in mV. These rates were used to predict steady state inactivation (*dashed line*, see text), which agrees well with the data (*closed squares*). (*B*) YY/QQ channels. τ_c and τ_{rec} do not agree with the theory used for WT channels. Steady state inactivation is superimposed with its best-fit Boltzmann curve (see Fig. 2 *B*).

each voltage were used to predict the steady state inactivation (*dashed line*). The accuracy of this prediction for WT channels shows that the kinetics of inactivation are reasonably well represented by a first order process. The ascending and descending slopes of the bell-shaped curve are the expectations of a model in which inactivation is rate limited by the movement, across the membrane field, of a gate with a charge of 4.40 e_0. Because the microscopic rate constant for inactivating, for example from an open state of a sodium channel, is much faster than macroscopic rates of inactivation (Aldrich, Corey, and Stevens, 1983; Vandenberg and Horn, 1984), the slow time constant τ_c shown in Fig. 4 *A* may represent a slow conformational change that precedes a rapid entry into an inactivated state.

Similar plots for YY/QQ fail to show this simple relationship between time constants and steady state inactivation (Fig. 4 *B*), especially because $\tau_c < \tau_{rec}$ in the voltage range where our measurements overlap. This suggests that a single conformational transition is not the rate-limiting factor underlying inactivation in these mutant channels. Indeed the time constants τ_{rec} and τ_c are both much smaller in YY/QQ than in WT channels. If WT inactivation is coupled to a slow conformational transition (e.g., a closed–closed transition in the activation pathway), this transition is either faster in YY/QQ and no longer rate-limiting, or else the link between this slow transition and inactivation is broken in YY/QQ.

Effect of Tyrosine Mutations on Activation

Our data show a reduced voltage dependence of inactivation in the mutant YY/QQ. Since it is believed that inactivation derives most of its voltage dependence from being coupled to activation voltage sensors (Armstrong, 1981; Bezanilla, 1985; Patlak, 1991; Keynes, 1994), mutations that uncouple inactivation from activation might also be expected to alter activation rates. We examined the effects of YY/QQ on activation, using both whole-cell and single-channel sodium currents.

Fig. 5 *A* shows that the peak current-voltage relationship for whole-cell sodium current is shifted in the depolarizing direction for the YY/QQ mutant. A normalized conductance-voltage (*G-V*) plot (Fig. 5 *B*) shows a 5.1-mV depolarizing shift for YY/QQ, as well as a decrease in the slope of a Boltzmann fit to these data. The decrease in slope is equivalent to a difference of 0.8 e_0. The depolarizing shift in YY/QQ could be due to a decreased rate of activation at negative voltages. Alternatively it could be a consequence of increased rate constants for inactivation, which could reduce the peak conductance. To study the rapid kinetics of activation, we obtained whole-cell currents at a decreased temperature (15°C). Fig. 6 *A* shows that YY/QQ channels open more rapidly at −40 mV than WT channels. We quantified this observation by plotting the half times for activation over a 100-mV voltage range. Fig. 6 *B* shows that the macroscopic kinetics of activation are slower and more voltage dependent for WT than for YY/QQ channels at voltages more negative than −20 mV.

Although these results suggest that the voltage dependence and kinetics of activation are altered in YY/QQ, all of the data are influenced by inactivation from closed states. To examine one of the activation steps with little contamination from inactivation, we measured the rate and voltage dependence of tail current decay. At voltages more negative than −70 mV, where channels are not expected to reopen

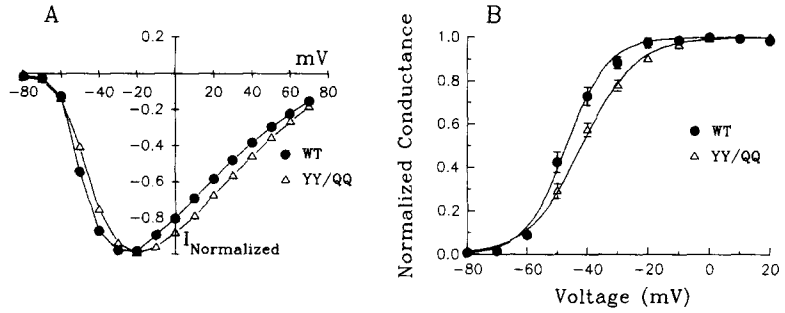

FIGURE 5. Activation. (*A*) Normalized peak current-voltage (*I-V*) relationship for 14 WT and 13 YY/QQ cells. Standard error bars are smaller than the symbols. (*B*) Normalized conductance-voltage relationship for the *I-V* curves. Boltzmann curves have slopes of 6.7 ± 0.7 mv (*WT*) and 8.9 ± 0.3 mV (*YY/QQ*). The midpoints are −46.9 ± 7.6 mV (*WT*) and −41.8 ± 0.3 mv (*YY/QQ*).

after closing (Fig. 5 *B*), and where the deactivation rate constant is likely to be faster than the inactivation rate constant from the open state (however, see Aldrich and Stevens, 1987), the inverse of the deactivation time constant is an estimate of the transition rate between the open state and its preceding closed state in the activation pathway. Fig. 6 *C* shows superimposed current traces with indistinguishable deactivation kinetics between WT and YY/QQ at −90 mV, and Fig. 6 *D* shows that deactivation time constants have an exponential voltage dependence in both mutant and WT. These time constants are marginally, but not significantly, larger in the mutant ($P \cong 0.09$, *F* test), showing that the open-to-closed transition in the activation pathway is relatively insensitive to the YY/QQ mutations in this voltage range. Although this double mutation does not strongly affect a deactivation rate constant, our data cannot exclude the possibility that other transitions in the activation pathway are altered.

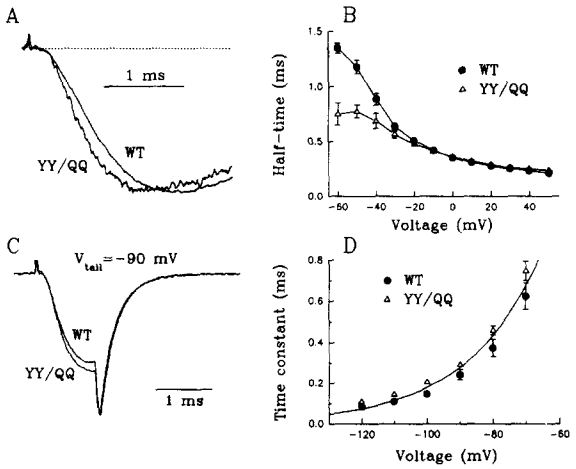

FIGURE 6. Macroscopic kinetics of activation and deactivation. (*A*) Activation time course at −40 mV at 15°C. (*B*) Half-times to peak current, 15°C. (*C*) Scaled, superimposed tail currents of WT and YY/QQ currents at −90 mV, after a 1.05-ms activating step to −20 mV, 15°C. (*D*) Time constants for deactivation at 15°C. Tail currents fit to single exponential relaxations (O'Leary and Horn, 1994). The time constants have an exponential voltage dependence, equivalent to 1.15 ± 0.07 e_0.

Single-Channel Properties

One of the striking features of the currents of YY/QQ is that τ_h is constant over a voltage range (−50 to 0 mV) where channel opening is steeply voltage dependent (Figs. 1 *B* and 5 *B*). Aldrich et al. (1983) showed, over a similar voltage range, that τ_h for sodium channels in neuroblastoma cells is largely determined by the latency for a channel to open after a depolarization. Our macroscopic current data suggest, therefore, that the first latency distribution is less voltage dependent in YY/QQ than in WT channels. To explore this idea we obtained single-channel recordings from cell-attached patches of transfected cells at −40 and −20 mV (Fig. 7). The single-channel currents of WT and YY/QQ have, on the average, comparable open times, number of openings per burst, probability of not opening during a depolarization (P_{blank}), and peak open probability (Table I). However there is a clear difference between the first latency distributions of WT and YY/QQ channels. The median first latencies are significantly shorter and less voltage dependent for mutant channels (Fig. 8, *A* and *B*, Table I). In WT channels, the first latency increased 2.7-fold between −20 and −40 mV, compared with 1.6-fold for YY/QQ (Table I). The ensemble-averaged currents show, as in whole-cell recordings, that τ_h is less voltage dependent in the mutant (Fig. 8, *C* and *D*, Table I). The fact that peak open

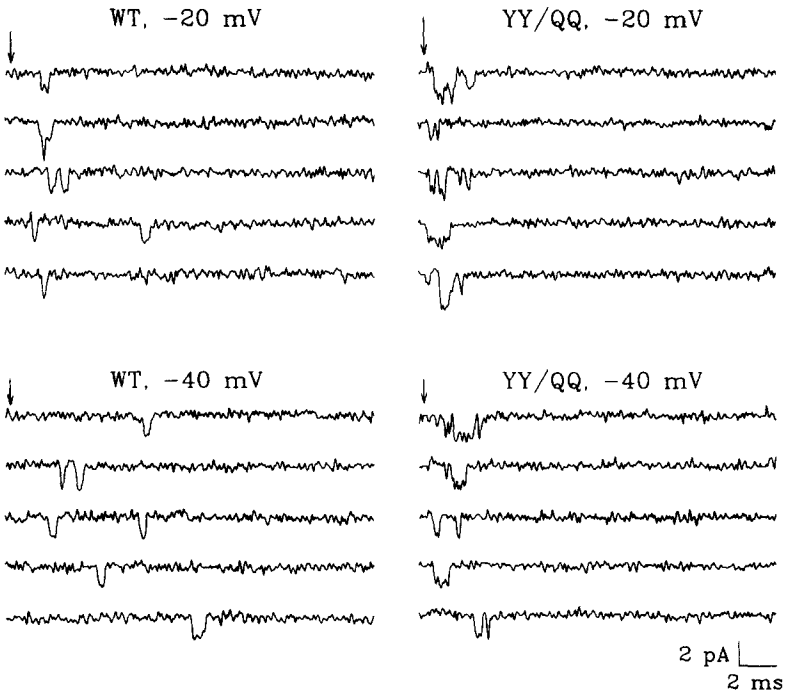

FIGURE 7. Single-channel currents. Selected examples of single-channel currents at −20 and −40 mV (*arrows*) from cell-attached patches; holding potential, −120 mV; low-pass filter, 3.1 kHz. WT and YY/QQ patches had two and four channels, respectively.

TABLE I

Analysis of Single Channels in Cell-attached Patches

	V	WT	YY/QQ	*P*-value
	mV			
Mean open	-20	303 ± 16	338 ± 18	>0.1
time (μs)	-40	252 ± 12	268 ± 17	>0.2
Burst number	-20	1.38 ± 0.08	1.46 ± 0.09	>0.5
	-40	1.36 ± 0.06	1.33 ± 0.06	>0.5
Peak	-20	0.132 ± 0.023	0.149 ± 0.015	>0.5
P_{open}	-40	0.045 ± 0.013	0.059 ± 0.012	>0.2
Median first	-20	0.71 ± 0.03	0.57 ± 0.03	<0.01*
latency (ms)	-40	1.92 ± 0.20	0.94 ± 0.07	<0.001*
P_{blank}	-20	0.590 ± 0.044	0.638 ± 0.031	>0.2
	-40	0.658 ± 0.064	0.615 ± 0.063	>0.2
τ_h (ms)	-20	0.83 ± 0.07	0.97 ± 0.05	>0.1
	-40	2.33 ± 0.25	1.18 ± 0.14	<0.02*

Patches contained one to four channels. Values are mean ± SEM for seven WT patches and 10 YY/QQ patches. The means and variances were weighted according to the number of depolarizations and the number of channels (N) in each patch. Mean open time, number of openings per burst, and first latencies corrected for N, were calculated as described previously (Chahine et al., 1994). The probability that a channel will inactivate without opening, P_{blank}, is estimated from the N^{th} root of the fraction of blank records. Peak open probability and τ_h were obtained from ensemble-averaged currents. *P* values were obtained by an unpaired, two-sided *t* test.

probability is not significantly affected by YY/QQ mutations (Table I) does not contradict the effects observed on *G-V* curves (Fig. 5 *B*). The *G-V* curves are arbitrarily scaled and only indirectly provide information on the voltage dependence of open probability.

We observe increased macroscopic rates of inactivation from closed states at negative voltages. This could be a consequence of either or both of two effects of the double mutation. One possibility is that inactivation rate constants from closed states are increased in mutant channels. This would predict a reduction of the peak open probability, a result inconsistent with our data (Table I). The second possibility is that activation rate constants are increased. The shortened first latencies in the mutant could be due to such an effect. Accelerated movement along the activation pathway could cause a more rapid inactivation at very negative voltages, due to the coupling between activation and inactivation. This second possibility predicts an increase in the peak open probability in mutant channels, a result also inconsistent with our data. Therefore, both activation and inactivation rate constants must be affected in mutant channels. Our data indicate that, at voltages negative to −20 mV, rate constants both from closed-to-open states, and from closed-to-inactivated states, are increased in YY/QQ mutants.

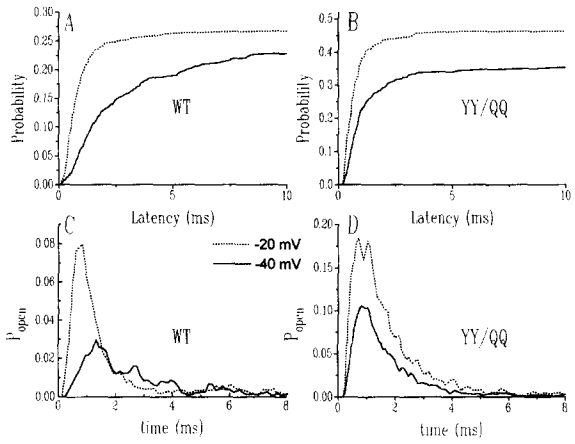

FIGURE 8. Analysis of single-channel data of patches in Fig. 7. (*A*) First latency distributions for the WT patch, corrected for the number of channels. In this patch the median first latency was 0.68 ms (−20 mV) and 1.8 ms (−40 mV). (*B*) Corrected first latency distributions for the YY/QQ patch. In this patch the median first latency was 0.56 ms (−20 mV) and 0.84 ms (−40 mV). (*C*) Ensemble average open probability for the WT patch, using 589 (−20 mV) and 585 (−40 mV) depolarizations. (*D*) Ensemble average open probability for the YY/QQ patch, using 300 (−20 mV) and 597 (−40 mV) depolarizations.

DISCUSSION

We have examined the role of a pair of adjacent tyrosine residues on the cytoplasmic D3–D4 linker of human cardiac sodium channels. These residues are located seven residues downstream from a trio of hydrophobic residues (IFM) known to be important for the rapid inactivation of sodium channels of brain and heart (West et al., 1992; Hartmann et al., 1994). Substitution of glutamines for these two adjacent tyrosines accelerates the decay of sodium currents after depolarizations to voltages more negative than −30 mV. In contrast to WT channels, where the time constant τ_h of inactivation decreases strongly with depolarization, τ_h in YY/QQ channels increases slightly with depolarization (Fig. 2 *A*). The kinetics of recovery from inactivation are faster in mutant than WT channels and have a decreased voltage dependence (Fig. 2 *D*). Despite these marked differences in the voltage dependence and kinetics of macroscopic inactivation between WT and mutant channels, the midpoints of steady state inactivation are not significantly different (Fig. 2 *B*).

The YY/QQ mutations, which are located on the putative inactivation gate of sodium channels, also alter activation. Effects on activation have also been observed for other mutations in the D3–D4 linker (Moorman et al., 1990; Patton et al., 1992). The YY/QQ mutations shift the *G-V* relationship toward more depolarized voltages and reduce its voltage dependence (Fig. 5 *B*). Shifts in *G-V* curves are usually attributed to changes in the voltage dependence of activation, although changes in rates of inactivation may also play a role. The kinetics of whole-cell current activation are also affected by YY/QQ mutations, being faster at voltages more negative than −20 mV (Fig. 6, *A* and *B*). Consistent with this observation, the median first latencies for single-channel openings at −40 mV are twofold larger in WT than mutant channels (Table I). These data support the idea that YY/QQ mutations affect rate constants underlying both activation and inactivation. Direct ef-

fects on activation rate constants could explain our result that the delay preceding the inactivation of the channels at −30 mV is significantly reduced by the YY/QQ mutations (Fig. 3 *D*). This delay is believed to reflect the movement of sodium channels through closed conformations that precede both opening and inactivation (Goldman and Schauf, 1972; Bezanilla and Armstrong, 1977). Mutant channels evidently traverse this pathway more rapidly than WT channels at negative voltages.

Although the aforementioned data suggest that activation rate constants are altered in YY/QQ channels, changes of rate constants leading to inactivated states can also alter the apparent voltage dependence and kinetics of activation. Because we observe increased macroscopic rates of inactivation at negative voltages without a significant change in peak open probability, YY/QQ mutations must affect rate constants of the activation pathway as well as those between closed and inactivated states. This conclusion is strengthened by maximum likelihood estimates of rate constants from single-channel data at −40 mV, using several different gating models (O'Leary and Horn, unpublished observations).

Our macroscopic and single-channel data suggest an explanation for the lack of voltage dependence of τ_h in YY/QQ channels. After a depolarization, a mutant channel can bail out of the activation pathway by inactivating more readily from a closed state, due both to an increase in the rate of closed-channel inactivation and an increase in activation rate constants. As a consequence, the first latencies will decrease in the mutant. This is explained in part by the fact that the only channels that will open, and therefore contribute to the first latency distribution, must do so rapidly before inactivating from closed states. A larger rate of inactivation from a closed state will result in first latencies with a decreased voltage dependence, compared to WT (unpublished simulations). The decrease in magnitude and voltage dependence of the first latencies in YY/QQ channels causes τ_h to be faster and less voltage dependent at voltages more negative than −20 mV.

Comparison with Previous Results

The effects of these tyrosine mutations contrast strongly with previously described mutations of the neighboring aromatic residue phenylalanine in the IFM cluster (West et al., 1992; Hartmann et al., 1994). In particular, phenylalanine F1486 of hH1 plays a dominant role in inactivation at negative voltages, because the mutation F1486Q drastically reduces inactivation from closed states, and also causes a large depolarizing shift in steady state inactivation (Hartmann et al., 1994). The repetitive openings observed with F1486Q indicate that inactivation is destabilized by this mutation. Although the YY/QQ mutant has altered rates of inactivation, the "burstiness" of channels is not increased and the midpoint of steady state inactivation is only moderately affected (Fig. 2 *B*), pointing out the different roles played by these aromatic residues in the D3–D4 linker. The equilibrium between closed and inactivated states depends on F1486, whereas Y1494 and Y1495 play a significant role in the rates of inactivation with little contribution to the relative free energies of closed and inactivated states. Because these tyrosines reside on the putative cytoplasmic inactivation gate, it is tempting to explain the effects of the double mutation by a conformational change of the inactivation gate that decreases the activation energy barrier for its interaction with its receptor. This would increase the

rates of both inactivation and recovery from inactivation in the mutant. However this interpretation cannot easily explain the decreased rate of inactivation of YY/QQ channels at more positive voltages or the significant loss of voltage dependence of τ_h, τ_c, and τ_{rec}. Furthermore, this hypothesis does not yield a simple explanation for the effects of YY/QQ on activation rate constants. We explore a model below that can account for the numerous consequences of YY/QQ mutations.

Balls and Chains and Hinged Lids

The "ball-and-chain" model was originally proposed to explain the inactivation of sodium channels in squid axons (Armstrong and Bezanilla, 1977). This model assumes that depolarization causes activation gates to move, which creates a favorable binding site for a tethered cytoplasmic inactivation particle that can act as an open channel blocker. This mechanism may account entirely for the coupling between membrane potential and so-called *N*-type inactivation in potassium channels (Hoshi, Zagotta, and Aldrich, 1990; Zagotta, Hoshi, and Aldrich, 1990; Demo and Yellen, 1991; Murrell-Lagnado and Aldrich, 1993*a*; Murrell-Lagnado and Aldrich, 1993*b*). Because the cytoplasmic D3–D4 linker of sodium channels is tethered at both ends, a latching hinged-lid mechanism of inactivation has been proposed in analogy with the ball-and-chain model (West et al., 1992). However, there is little evidence for this type of mechanism in sodium channels, except that mutations of the D3–D4 linker affect inactivation. In potassium channels, for example, cytoplasmic open channel blockers interfere with *N*-type inactivation (Choi, Aldrich, and Yellen, 1991). Similar results are not obtained for sodium channels (O'Leary and Horn, 1994). Furthermore, the inactivation of potassium channels lacking a tethered inactivation particle may be restored with soluble ball peptides (Zagotta et al., 1990; Demo and Yellen, 1991; Murrell-Lagnado and Aldrich, 1993*a*,*b*). Comparable experiments with sodium channels (Eaholtz, Scheuer, and Catterall, 1994; Eaholtz, Zagotta, and Catterall, 1995) produce, at best, a voltage-dependent open-channel block distinctly different from normal inactivation, which is thought to have little inherent voltage dependence. Another clear difference between *N*-type inactivation in potassium channels and inactivation of sodium channels is that electrostatic interactions are important for the reaction between the inactivation particles of potassium channels and their binding site (Murrell-Lagnado and Aldrich, 1993*b*). This is apparently not the case for sodium channels (Moorman et al., 1990; West et al., 1992).

N-type inactivation in potassium channels behaves as if the tethered inactivation particles, which number four in homotetrameric channels (MacKinnon, Aldrich, and Lee, 1993), are fully dissociated from the core of the channel until the channel inactivates. The binding of one of the four inactivation particles, or of an exogenous ball peptide molecule, causes inactivation. Removing the amino-terminal inactivation particles by deletion has no effect on activation gating during a depolarization (Hoshi et al., 1990), consistent with the idea that the inactivation particles are not associated with the channel core except when the channel is inactivated. Furthermore, the rate of recovery from *N*-type inactivation does not depend on the number of inactivation particles in heteromeric potassium channels (MacKinnon et al., 1993; Gomez-Lagunas and Armstrong, 1995), again showing that the only in-

activation particle that interacts with gating mechanisms is the one bound in its site. However the activation gating charge is "immobilized" in an inactivated potassium channel (Perozo, Papazian, Stefani, and Bezanilla, 1992), which is evidence that an inactivation particle, when bound in its site, is in contact with the channel core where it can interact with activation gates.

By analogy with potassium channels, the phenylalanine in the IFM triplet of sodium channels may bind to a site on the core of the channel protein, causing inactivation (West et al., 1992). Depolarization could induce the formation of a high affinity docking site for this phenylalanine. We believe that this change of affinity accompanies rapid, voltage-dependent transitions near the beginning of the activation pathway, and that mutations of phenylalanine F1486 alter this voltage-dependent affinity. In stark contrast with potassium channels, YY/QQ mutations in the putative inactivation gate of sodium channels alter rate constants for activation, indicating an association between activation and inactivation gates, even when the channel is not inactivated. This association affects both the activation gating in WT channels and the voltage dependence and kinetics of inactivation.

A Model for Sodium Channel Inactivation

We postulate that a depolarization has two effects on the process of inactivation. The first, as discussed above, is the rapid creation of a favorable binding site for the cytoplasmic inactivation gate. The second is a slower conformational change in the D3–D4 linker, due to its association with a voltage sensor in the core of the channel protein. We believe that this molecular link contributes to the voltage dependence of the kinetics of both inactivation and recovery from inactivation, and that the YY/QQ mutations disrupt this link. The most compelling evidence for this disruption is that the voltage dependence of inactivation, however it is measured (Figs. 2, 3, and 8; Table I), is reduced in YY/QQ channels. Because the relative free energy of closed and inactivated states is not altered markedly by YY/QQ mutations, it is likely that the affinity of IFM for its putative binding site is unaltered. However, the rates of association and dissociation of IFM are increased in YY/QQ channels at voltages more negative than −20 mV, as if these mutations disrupt the normal coupling between a slow conformational transition in the activation pathway and the inactivation process. In WT channels this slow transition is rate limiting, and can account for the rates and voltage dependence of inactivation (Fig. 4 *A*). One effect of the disruption of coupling is that the activation rates are greater in YY/QQ than in WT channels at voltages more negative than −20 mV (Fig. 6), perhaps because activation gating transitions are no longer encumbered by the inactivation gate. The increase in rate of activation in YY/QQ is partly responsible for the decrease in the lag for development of inactivation after a depolarization (Fig. 3).

We have restricted most of our discussion to voltages more negative than −30 mV, in part because of the more dramatic differences between mutant and WT channels for these voltages. This is also the range where the voltage dependence of both activation and inactivation is most pronounced. At potentials more depolarized than −30 mV the macroscopic inactivation rate of YY/QQ is slower than in WT channels, presumably because the residue F1486 of the mutant is not delivered effectively to its site, even after the activation gates are fully open. The hampered

ability of the "ball" of YY/QQ to bind to its site at positive voltages could explain the gradual increase in τ_h with depolarization (Fig. 2 *A*), because mutant channels tend to get trapped in the open state, due to the voltage dependence of the rate constant leading from the open state to a closed state in the activation pathway. This conceptual model provides a plausible explanation for the difference in recovery from inactivation between WT and YY/QQ channels. First, the molecular association between the inactivation gate and a voltage sensor in the core of the channel protein promotes a more stable binding of the inactivation gate, leading to slower recovery from inactivation in the WT. Furthermore, because of the association with a voltage sensor, recovery should be more voltage dependent in WT than in YY/QQ channels, consistent with our observations.

Although our data give strong evidence for an association between the D3–D4 linker and an activation voltage sensor, our interpretation of the effects of YY/QQ mutations, i.e., a disruption of this link, is only one possibility. Our data cannot distinguish this hypothesis from those in which the link is maintained, but is functionally altered. Any mechanistic interpretation, however, must be able to account for the alterations in both activation and inactivation gating. To simplify such an interpretation, we are currently exploring the effects of YY/QQ mutations on channels that cannot inactivate, due to IFM/QQQ mutations.

Our data suggest a fundamental difference between potassium and sodium channels in the coupling mechanisms between activation and inactivation. Although we believe that a rapid, voltage-dependent change in affinity for a cytoplasmic inactivation particle occurs in both types of channels, the inactivation gate of sodium channels is also linked with activation voltage sensors when the channel is not inactivated. Because the conformational transitions, both entering and leaving an inactivated state, are rate limiting in WT channels, our data are suggestive of a gating model containing parallel fast and slow pathways. The more rapid transitions involve activation and deactivation; inactivation is slower in both onset and recovery. The YY/QQ mutations specifically disrupt the association between slow conformational transitions and inactivation. This type of parallel model (Keynes, 1990; Patlak, 1991; Keynes, 1994; Kuo and Bean, 1994; Schoppa and Sigworth, 1994; Zagotta, Hoshi, and Aldrich, 1994) is in accord with the presence of the four S4 segments in both potassium channels and sodium channels. The mechanism by which voltage-dependent conformational changes of the channel core are transmitted to the inactivation gate of sodium channels remains a mystery and includes the possibility that the tyrosines directly contribute to the molecular link. The absence of voltage dependence of τ_h for YY/QQ at negative potentials is reminiscent of a similar behavior seen in naturally occurring mutants associated with the disease paramyotonia congenita (Chahine et al., 1994). These natural mutations, which affect both activation and inactivation, are found in the S4 segment of D4. In fact this phenotype, a voltage-independent τ_h at negative membrane potentials, is only observed for S4 mutations of D4, and not for equivalent mutations in other domains (Chen, Santarelli, Zhang, Horn, and Kallen, 1995), suggesting that this highly charged transmembrane segment is the voltage sensor in this coupling mechanism.

We thank Vincent Santarelli for help with transfections and tissue culture, and Drs. J. B. Patlak,

M. L. Covarrubias, and C. Deutsch for comments on the manuscript.

Supported by NIH grants AR41,691 (R. Horn) and AR41,762 (R. G. Kallen), and grants from the American Heart Association (R. G. Kallen) and the Research Foundation of the University of Pennsylvania (R. G. Kallen).

Original version received 2 March 1995 and accepted version received 8 May 1995.

REFERENCES

Aldrich, R. W., D. P. Corey, and C. F. Stevens. 1983. A reinterpretation of mammalian sodium channel gating based on single channel recording. *Nature.* 306:436–441.

Aldrich, R. W., and C. F. Stevens. 1987. Voltage-dependent gating of single sodium channels from mammalian neuroblastoma cells. *Journal of Neuroscience.* 7:418–431.

Armstrong, C. M. 1981. Sodium channels and gating currents. *Physiological Reviews.* 61:644–683.

Armstrong, C. M., and F. Bezanilla. 1977. Inactivation of the sodium channel. II. Gating current experiments. *Journal of General Physiology.* 70:567–590.

Bezanilla, F. 1985. Gating of sodium and potassium channels. *Journal of Membrane Biology.* 88:97–111.

Bezanilla, F., and C. M. Armstrong. 1977. Inactivation of the sodium channel. I. Sodium current experiments. *Journal of General Physiology.* 70:549–566.

Chahine, M., A. L. George, Jr., M. Zhou, S. Ji, W. Sun, R. L. Barchi, and R. Horn. 1994. Sodium channel mutations in paramyotonia congenita uncouple inactivation from activation. *Neuron.* 12:281–294.

Chen, L.-Q., V. Santarelli, P. Zhang, R. Horn, and R. G. Kallen. 1995. Unique role for the S4 segment of domain 4 of sodium channels. *Biophysical Journal.* 68:A156. (Abstr.)

Choi, K. L., R. W. Aldrich, and G. Yellen. 1991. Tetraethylammonium blockade distinguishes two inactivation mechanisms in voltage-activated K^+ channels. *Proceedings of the National Academy of Sciences, USA.* 88:5092–5095.

Demo, S. D., and G. Yellen. 1991. The inactivation gate of the *Shaker* K^+ channel behaves like an open-channel blocker. *Neuron.* 7:743–753.

Eaholtz, G., T. Scheuer, and W. A. Catterall. 1994. Restoration of inactivation and block of open sodium channels by an inactivation gate peptide. *Neuron.* 12:1041–1048.

Eaholtz, G., W. N. Zagotta, and W. A. Catterall. 1995. Kinetic analysis of time-dependent open channel block by an inactivation gate peptide of non-inactivating type IIa sodium channels. *Biophysical Journal.* 68:A159. (Abstr.)

Gellens, M. E., A. L. George, Jr., L.-Q. Chen, M. Chahine, R. Horn, R. L. Barchi, and R. G. Kallen. 1992. Primary structure and functional expression of the human cardiac tetrodotoxin-insensitive voltage-dependent sodium channel. *Proceedings of the National Academy of Sciences, USA.* 89:554–558.

Gillespie, J. I., and H. Meves. 1980. The time course of sodium inactivation in squid giant axons. *Journal of Physiology.* 299:289–308.

Goldman, L., and J. L. Kenyon. 1982. Delays in inactivation development and activation kinetics in Myxicola giant axons. *Journal of General Physiology.* 80:83–102.

Goldman, L., and C. L. Schauf. 1972. Inactivation of the sodium current in Myxicola giant axons; evidence for coupling to the activation process. *Journal of General Physiology.* 59:659–675.

Gomez-Lagunas, F., and C. M. Armstrong. 1995. Inactivation in *Shaker* B K^+ channels: a test for the number of inactivating particles on each channel. *Biophysical Journal.* 68:89–95.

Hartmann, H. A., A. A. Tiedeman, S.-F. Chen, A. M. Brown, and G. E. Kirsch. 1994. Effects of III-IV linker mutations on human heart Na^+ channel inactivation gating. *Circulation Research.* 75:114–122.

Hodgkin, A. L., and A. F. Huxley. 1952. A quantitative description of membrane current and its appli-

cation to conduction and excitation in nerve. *Journal of Physiology.* 117:500–544.

Hoshi, T., W. N. Zagotta, and R. W. Aldrich. 1990. Biophysical and molecular mechanisms of *Shaker* potassium channel inactivation. *Science.* 250:533–538.

Keynes, R. D. 1990. A series-parallel model of the voltage-gated sodium channel. *Proceedings of the Royal Society of London B.* 240:425–432.

Keynes, R. D. 1994. The kinetics of voltage-gated ion channels. *Quarterly Reviews of Biophysics.* 27:339–434.

Kuo, C.-C., and B. P. Bean. 1994. Na^+ channels must deactivate to recover from inactivation. *Neuron.* 12:819–829.

MacKinnon, R., R. W. Aldrich, and A. W. Lee. 1993. Functional stoichiometry of *Shaker* potassium channel inactivation. *Science.* 262:757–759.

Margolskee, R. F., B. McHendry-Rinde, and R. Horn. 1993. Panning transfected cells for electrophysiological studies. *Biotechniques.* 15:906–911.

Moorman, J. R., G. E. Kirsch, A. M. Brown, and R. H. Joho. 1990. Changes in sodium channel gating produced by point mutations in a cytoplasmic linker. *Science.* 250:688–691.

Murrell-Lagnado, R. D., and R. W. Aldrich. 1993*a*. Interactions of amino terminal domains of *Shaker* K channels with a pore blocking site studied with synthetic peptides. *Journal of General Physiology.* 102:949–975.

Murrell-Lagnado, R. D., and R. W. Aldrich. 1993*b*. Energetics of *Shaker* K channels block by inactivation peptides. *Journal of General Physiology.* 102:977–1003.

O'Leary, M. E., and R. Horn. 1994. Internal block of human heart sodium channels by symmetrical tetra-alkylammoniums. *Journal of General Physiology.* 104:507–522.

Patlak, J. 1991. Molecular kinetics of voltage-dependent Na^+ channels. *Physiological Reviews.* 71:1047–1080.

Patton, D. E., J. W. West, W. A. Catterall, and A. L. Goldin. 1992. Amino acid residues required for fast Na^+-channel inactivation: charge neutralizations and deletions in the III-IV linker. *Proceedings of the National Academy of Sciences, USA.* 89:10905–10909.

Perozo, E., D. M. Papazian, E. Stefani, and F. Bezanilla. 1992. Gating currents in *Shaker* K^+ channels. Implications for activation and inactivation models. *Biophysical Journal.* 62:160–168.

Rogart, R. B., L. L. Cribbs, L. K. Muglia, D. D. Kephart, and M. W. Kaiser. 1989. Molecular cloning of a putative tetrodotoxin-resistant rat heart Na^+ channel isoform. *Proceedings of the National Academy of Sciences, USA.* 86:8170–8174.

Rojas, E., and C. M. Armstrong. 1971. Sodium conductance activation without inactivation in pronase-perfused axons. *Nature New Biology.* 229:177–178.

Schoppa, N. E., and F. J. Sigworth. 1994. Activation model for wild-type and V2 mutant *Shaker* potassium channels. *Biophysical Journal.* 66:A22.(Abstr.)

Sigworth, F. J. 1993. Voltage gating of ion channels. *Quarterly Reviews of Biophysics.* 27:1–40.

Stühmer, W., F. Conti, H. Suzuki, X. D. Wang, M. Noda, N. Yahagi, H. Kubo, and S. Numa. 1989. Structural parts involved in activation and inactivation of the sodium channel. *Nature.* 339:597–603.

Vandenberg, C. A., and R. Horn. 1984. Inactivation viewed through single sodium channels. *Journal of General Physiology.* 84:535–564.

West, J. W., D. E. Patton, T. Scheuer, Y. Wang, A. L. Goldin, and W. A. Catterall. 1992. A cluster of hydrophobic amino acid residues required for fast Na^+-channel inactivation. *Proceedings of the National Academy of Sciences, USA.* 89:10910–10914.

Zagotta, W. N., T. Hoshi, and R. W. Aldrich. 1990. Restoration of inactivation in mutants of *Shaker* potassium channels by a peptide derived from ShB. *Science.* 250:568–571.

Zagotta, W. N., T. Hoshi, and R. W. Aldrich. 1994. *Shaker* potassium channel gating. III. Evaluation of kinetic models for activation. *Journal of General Physiology.* 103:321–362.